

Accelerated Reinforcement Learning Algorithms with Nonparametric Function Approximation for Opportunistic Spectrum Access

Theodoros Tsiligkaridis, *Member, IEEE*, David Romero

Abstract—We study the problem of throughput maximization by predicting spectrum opportunities using reinforcement learning. Our kernel-based reinforcement learning approach is coupled with a sparsification technique that efficiently captures the environment states to control dimensionality and finds the best possible channel access actions based on the current state. This approach allows learning and planning over the intrinsic state-action space and extends well to large state and action spaces. For stationary Markov environments, we derive the optimal policy for channel access, its associated limiting throughput, and propose a fast online algorithm for achieving the optimal throughput. We then show that the maximum-likelihood channel prediction and access algorithm is suboptimal in general, and derive conditions under which the two algorithms are equivalent. For reactive Markov environments, we derive kernel variants of Q-learning, R-learning and propose an accelerated R-learning algorithm that achieves faster convergence. We finally test our algorithms against a generic reactive network. Simulation results are shown to validate the theory and show the performance gains over current state-of-the-art techniques.

Index Terms—Reinforcement Learning, Opportunistic Spectrum Access, Channel Access Policy, Kernel, Throughput Maximization.

I. INTRODUCTION

The FCC has recognized that conventional static spectrum allocation methods lead to spectrum being under-utilized [1]. RF spectrum is a highly valued commodity; 65MHz of spectrum was auctioned in the US (AWS-3) for \$40B. The FCC realizes the huge demand for spectrum and its inefficient use today, and is creating the Innovation Band around 100MHz wide at 3.5GHz to allow cognitive radios to access spectrum there opportunistically. Currently, there is no established cognitive solution for use of this band, providing an opportunity for researchers to shape how spectrum is utilized in the future. The need for intelligent algorithms for autonomous spectrum and power allocation across different nodes in networks has been growing in the last decade. Opportunistic spectrum access (OSA) can be used to efficiently exploit spectrum opportunities by allowing secondary users (SU) to find and access parts of the spectrum such that they cause limited interference to

primary users (PU) [2]. OSA has become important recently as spectrum bands are becoming more congested.

In OSA, nodes within a cognitive radio network (CRN) collect spectrum data and must find efficient ways to access spectrum while avoiding collisions with other networks in real-time. Much of the current literature on OSA deals with its underlying CRN architecture and implementation [3], [4], [5], [6], [7], performance optimization and MAC protocol design [8], [9], [10], [11], [12], [13], but little effort has been given to developing *learning*-based approaches that are both effective and practical when dealing with exploiting opportunities in *unknown* RF environments that are capable of reacting to transmission actions being taken.

Many of the proposed learning algorithms based on hidden Markov models, neural networks, and other predictive models tend to require a prohibitive amount of computational resources to train, often require periodic retraining, and may require a very large number of parameters to capture relevant communication environments [14], [15]. Furthermore, even state-of-the-art deep learning models are sensitive to noise [16] and adversarial actions [17]. These problems prohibit the use of these algorithms in practical environments due to the amount of data and tight latency requirements. For spectrum prediction and exploitation, this data must be analyzed in real-time to be valuable for decision making.

In this paper, we develop novel machine learning algorithms to enable autonomous learning and increase spectrum efficiency in *unknown* and *dynamic* RF environments. The dynamic nature of the RF environment covers cases when taking actions lead to changes in the RF environment, i.e., colliding with a PU may force the PU to move to a different frequency band or backoff its data rate. Reinforcement learning (RL) provides a natural framework for model-free optimization with the goal of learning optimal channel access policies, in which radios learn by direct interaction with the environment. RL has been proposed for cognitive radio networks in the context of cooperative sensing [18], interference control [19], optimization of queueing systems [20], and spectrum management [21].

To learn a good spectrum access policy, radios must balance the exploration of the space of states and actions with the exploitation of an already learned policy [22]. The radios use acquired knowledge to choose actions (e.g., which channel to access) that maximize a cumulative reward (e.g., data rate). Learning a policy directly by interacting with the environment has the potential of providing adaptation capabilities and

This material is based upon work supported under Air Force Contract No. FA8721-05-C-0002 and/or FA8702-15-D-0001. Any opinions, findings, conclusions or recommendations expressed in this material are those of the author(s) and do not necessarily reflect the views of the U.S. Air Force.

Approved for Public Release, Distribution Unlimited.

T. Tsiligkaridis and D. Romero are with MIT Lincoln Laboratory, Lexington, MA 02421 USA (email: {ttsili,dlr}@ll.mit.edu).

significant savings in terms of computational complexity. This is coupled with a kernel-based framework for dimensionality reduction to capture the essential features of the communication environment. The advantages of this approach is that it is adaptive, flexible, and has low complexity. The approach is illustrated in Fig. 1. The algorithms developed in this

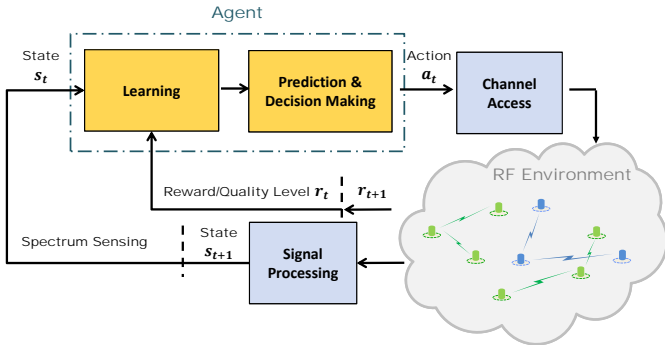


Fig. 1: Overview of reinforcement learning approach for opportunistic spectrum access.

work may also be useful for prediction in high-dimensional data, adaptive sensing, robotics and adaptive stochastic control problems.

A. Outline

The paper is organized as follows. The problem is formulated in Section II and the nonparametric function approximation modeling approach is described. Section III describes the dimensionality reduction algorithm and contains analysis that guides the selection of the kernel and approximation parameters. Section IV contains the performance analysis for the case of stationary Markov environments. Several kernel reinforcement learning algorithms are derived in Section V including the novel generalization of R-learning. Finally, numerical experiments are included in Section VI.

II. PROBLEM FORMULATION

We formulate the problem in the Markov decision process (MDP) context. We use the MDP $(\mathcal{S}, \mathcal{A}, R, \mathbf{P})$ to represent the dynamic communication environment of the green network (see Fig. 1), where \mathcal{S} is the state space, \mathcal{A} is the action space, R is the reward function and \mathbf{P} is the state-transition matrix. The policy of the MDP is a function $\pi : \mathcal{S} \rightarrow \mathcal{A}$ that maps state to actions. In the sequel we'll refer to secondary users as the *blue cognitive network* and primary users as the *green network*. The objective of the blue cognitive network is to find a channel access policy that maximizes its throughput while operating in the presence of and avoiding collisions with a green network. For simplicity, we consider a single blue receiver which may be used to model a single user link or a centralized controller that distributes a channel access schedule to user pairs via a control channel assuming all blue nodes are experiencing similar path losses.

A. State Space

The blue receiver is observing the states of a communication environment, $s_t \in \mathcal{S}$, which are power measurements of the received signals. We assume the available bandwidth is divided into K channels and the receiver can sense the full band yielding a state $s_t \in \mathbb{R}_+^K$ at each time instant. We assume that in the noiseless case, the state space \mathcal{S} is finite. We also assume full-duplex operation ¹.

B. Action Space

We assume, for simplicity, that the blue link is constrained to access one of the K channels at each time, and makes decisions $a_t \in \mathcal{A}$ about which channel to access based on the current state s_t . The action being taken a_t affects in general the evolution of the states. Of course, this assumption can be relaxed and the methods presented in the paper are still valid as long as the action space is parameterized appropriately. In the most general case where the blue link is capable of accessing up to K_a out of K channels at each time, action can be represented as binary vectors in a space \mathcal{A} of dimension $|\mathcal{A}| = \sum_{k=1}^{K_a} \binom{K}{k}$.

C. Transition Model

Under this dynamic model, the probability of being in the next state depends only on the current state s_t and the action taken a_t , i.e.,

$$P_{i,j}(a) = P(s_{t+1} = j | s_t = i, a_t = a)$$

For stationary environments the transitions do not depend on the actions, i.e., $P_{i,j}(a) = P_{i,j}$ for all $a \in \mathcal{A}$. To model reactive/adaptive environments, the transitions will depend on the actions being taken in general. We note that if the states evolve as a higher-order Markov chain, a new state space of higher dimension may be defined as first-order Markov and the same techniques may be applied.

D. Reward Model

The reward obtained when transitioning to state s_{t+1} as a result of taking action a_t in state s_t is given by the number of bits received successfully as a result of a single channel access and can be measured by an acknowledgment in practice. If the bit packet fails to be successfully received, a zero or negative reward is incurred due to the sensing overhead and the resulting collision with the green network. This can be written as:

$$r_t = \begin{cases} R(a_t), & \text{if channel } a_t \text{ is idle at state } s_{t+1} \\ -C_s, & \text{else} \end{cases}$$

where $R(a)$ is the number of bits successfully received when using channel a , which is upper bounded by the channel capacity. Note that we make the assumption that all packet losses for the blue network are due to channel access collisions.

¹The techniques can be extended to half-duplex by splitting each slot into a sensing and accessing time period.

E. Noise Modeling

In practice, there will be noise due to the receiver which makes the true states unobservable. The observation model in a AWGN channel over a subband k at time t is:

$$y_t(k) = z_t(k) + w_t(k)$$

where $w_t(k)$ is complex-valued white Gaussian noise with variance $\mathbb{E}|w_t(i)|^2 = \sigma_n^2$. The true power level is $|z_t(k)|^2$ and the noiseless state-vector is $\mathbf{p}_t = [|z_t(1)|^2, \dots, |z_t(K)|^2]^T$. Taking the power measurement of $y_t(k)$ and assuming independence between the transmitted signal and noise, we obtain:

$$\mathbf{s}_t = \mathbf{p}_t + \mathbf{n}_t$$

where $\mathbf{n}_t = [|w_t(1)|^2, \dots, |w_t(K)|^2]^T$. The noise distribution is exponential for each subband k , and due to independence across subbands, the multivariate distribution factors as

$$f(\mathbf{n}) = \prod_{k=1}^K \frac{1}{\sigma_n^2} e^{-n(k)/\sigma_n^2} I_{\{n(k) \geq 0\}}$$

The noise in our power measurements \mathbf{s}_t is highly non-Gaussian and concentrated on the positive orthant of the K -dimensional channel space.

F. Reinforcement Learning with Nonparametric Function Approximation

The objective is to find the optimal policy π^* that maximizes the long-term reward. The state-action value function may be defined to maximize the *discounted cumulative reward*:

$$Q^\pi(s, a) = \mathbb{E}^\pi \left[\sum_{t=0}^{\infty} \gamma^t r_t \mid s_0 = s, a_0 = a \right]$$

or to maximize the *long term average reward*:

$$Q^\pi(s, a) = \lim_{T \rightarrow \infty} \mathbb{E}^\pi \left[\frac{1}{T} \sum_{t=0}^T r_t \mid s_0 = s, a_0 = a \right]$$

The optimal state-action value function is

$$Q^*(s, a) = \max_{\pi} Q^\pi(s, a) \quad (1)$$

and the optimal policy is obtained as:

$$\pi^*(s) = \arg \max_{a \in \mathcal{A}} Q^*(s, a)$$

We adopt the framework of reinforcement learning with function approximation. Consider a data set generated from the MDP $\{(s_t, a_t, s_{t+1}, r_t)\}_{t=1}^T$ using the ϵ -greedy exploration method. Using the kernel-based approach of [22], [23], we model the state-action value functions of the MDP using a nonparametric nonlinear approximation:

$$Q(s, a) = \sum_{l=1}^L \alpha_l k((s, a), (s_l, a_l)) \quad (2)$$

where $k(\cdot, \cdot)$ is the kernel function and α_l is the coefficient associated with each state action pair (s_l, a_l) . We remark that the kernel can be thought of as an inner product in a Hilbert space \mathcal{H} , i.e., $k(x, x') = \langle \phi(x), \phi(x') \rangle$, and although the dimension of \mathcal{H} may be infinite and the nonlinear mapping

ϕ is unknown, all the computations can be performed in terms of inner products. We use the exponential kernel in this paper, i.e., $k(x, x') = \exp(-\frac{\|x-x'\|^2}{2\sigma^2})$, although other kernels may also be used in our approach.

The RL algorithms in this paper all have the same general form (see Fig. 1):

- (a) Choose action a_t based on ϵ -greedy policy, i.e.,

$$a_t = \begin{cases} \arg \max_{a \in \mathcal{A}} Q_t(s_t, a) + H_t(s_t, a), & \text{w.p. } 1 - \epsilon \\ \sim \text{unif}(\mathcal{A}), & \text{w.p. } \epsilon \end{cases}$$

where $Q_t(s_t, a) = \sum_l \alpha_l k((s_t, a), (s_l, a_l)) = \boldsymbol{\alpha}_t^T \mathbf{k}_t((s_t, a_t))$, $\mathbf{k}_t((s, a)) = [k((s, a), (s_1, a_1)), \dots, k((s, a), (s_L, a_L))]^T$ is a kernel-based vector, and $H_t(s_t, a)$ is a penalty function whose effect asymptotically vanishes, i.e., $\lim_{t \rightarrow \infty} H_t(s, a) = 0$.

- (b) Take action a_t , observe reward r_t and next state s_{t+1}
(c) Update state-action value function coefficients in expansion (2):

$$\boldsymbol{\alpha}_{t+1} = \boldsymbol{\alpha}_t + \eta_t (r_t + f_t - Q_t(s_t, a_t)) \mathbf{k}_t((s_t, a_t))$$

where f_t is a term that may depend on $\boldsymbol{\alpha}_t$ and s_{t+1} , and $\eta_t > 0$ is a step size parameter.

III. DIMENSIONALITY REDUCTION

A major issue that needs to be addressed when using the nonparametric model (2) is how to control its complexity without losing important information. The number of terms in the expansion (2) grow as the time horizon increases, making computational complexity intractable and reducing generalization performance.

We describe an online sparsification technique for deciding which terms to ignore and which terms to keep in the series expansion using approximate linear dependence (ALD) analysis [24], [23]. ALD analysis is a method for sequentially building a dictionary \mathcal{D} of representative feature vectors $\phi(x_i) = \phi((s_i, a_i))$. When a state-action pair $x = (s, a)$ is observed the ALD criterion is used to determine whether the corresponding feature vector $\phi((s, a))$ can be well approximated as a linear combination of feature vectors already included in \mathcal{D} . To understand more concretely how ALD is used in our approach, let the dictionary after testing $t-1$ samples be given by $\mathcal{D}_{t-1} = \{x_j = (s_j, a_j) : j = 1, \dots, L_{t-1}\}$. Given the new datum $x_t = (s_t, a_t)$, the test for whether to include x_t in the dictionary becomes:

$$\delta_t = \min_{\mathbf{c}} \left\| \sum_{j=1}^{L_{t-1}} c_j \phi(x_j) - \phi(x_t) \right\|^2 > \mu \quad (3)$$

where $\mu > 0$ is a parameter controlling the approximation error. Defining the kernel matrix as $\mathbf{K}_{t-1} = \{k(x_i, x_j)\}_{i,j=1}^{L_{t-1}}$ and the vector $\mathbf{k}_{t-1}(x_t) = [k(x_1, x_t), \dots, k(x_{L_{t-1}}, x_t)]^T$, we can express the optimal solution to (3) and its corresponding optimal value as:

$$\begin{aligned} \mathbf{c}_t &= \mathbf{K}_{t-1}^{-1} \mathbf{k}_{t-1}(x_t) \\ \delta_t &= k_{tt} - \mathbf{k}_{t-1}(x_t)^T \mathbf{c}_t \end{aligned} \quad (4)$$

where $k_{tt} \stackrel{\text{def}}{=} k(x_t, x_t)$. If $\delta_t \leq \mu$, then the dictionary remains the same, i.e., $\mathcal{D}_t = \mathcal{D}_{t-1}$, otherwise, the new state-action pair is added and $\mathcal{D}_t = \mathcal{D}_{t-1} \cup \{(s_t, a_t)\}$.

If we associate each term in the dictionary with a function $\phi(\cdot)$, where $k(x, x') = \langle \phi(x), \phi(x') \rangle$, the set of functions tends to be approximately linearly independent. This approach essentially sparsifies the kernel expansion in (2) by keeping relevant terms while ignoring terms that have been observed previously in the data stream and, more generally, can be well approximated by a linear combination of other terms in the dictionary.

A. Dictionary Size & Parameter Selection

It is known that if $k(\cdot, \cdot)$ is a continuous kernel function and the state and action spaces are compact, then for any training sequence $\{x_t = (s_t, a_t)\}_{t=1}^T$ and for any positive μ , the dictionary is finite [24]. In our setting, the action space is finite but the state space is infinite due to the presence of noise. However, the exponentially decaying tails of the noise distribution imply that the observed state space is compact with high probability.

Next, we provide a few criteria for choosing the parameters μ and σ . Assume that the states in the kernel domain, i.e., $\{\phi(s_i)\}_{i=1}^N$, are linearly independent (and thus distinct).

In the noiseless case, the ALD test should create a new element if two state-action pairs differ. This occurs iff for all $x_1 \neq x_2$:

$$\begin{aligned} \|\phi(x_1) - \phi(x_2)\|_2^2 > \mu &\Leftrightarrow 2(1 - k(x_1, x_2)) > \mu \\ &\Leftrightarrow e^{-\|x_1 - x_2\|_2^2 / (2\sigma^2)} < 1 - \frac{\mu}{2} \\ &\Leftrightarrow \|x_1 - x_2\|_2^2 > 2\sigma^2 \log\left(\frac{1}{1 - \frac{\mu}{2}}\right) \\ &\Leftrightarrow \|s_1 - s_2\|_2^2 + \|a_1 - a_2\|_2^2 > 2\sigma^2 \log\left(\frac{1}{1 - \frac{\mu}{2}}\right) \end{aligned}$$

This inequality holds if:

$$\min\{d_{\min}(\mathcal{S})^2, d_{\min}(\mathcal{A})^2\} > 2\sigma^2 \log\left(\frac{1}{1 - \frac{\mu}{2}}\right) \quad (5)$$

where $d_{\min}(\mathcal{S}) \stackrel{\text{def}}{=} \min_{s_1 \neq s_2} \|s_1 - s_2\|_2$ and $d_{\min}(\mathcal{A}) \stackrel{\text{def}}{=} \min_{a_1 \neq a_2} \|a_1 - a_2\|_2$ are the minimum distances between two elements in the state and action spaces, respectively. Given bounds on the minimum distances in states and actions, we can choose σ and μ jointly so that the inequality (5) holds.

Next, we consider a benchmark probability for creating a new element using ALD:

$$\begin{aligned} p_{\text{new}} &= \mathbb{P}\left(\|\phi((\mathbf{p} + \mathbf{n}, a)) - \phi((\mathbf{p}, a))\|_2^2 > \mu\right) \\ &= \mathbb{P}(2(1 - k(\mathbf{p} + \mathbf{n}, \mathbf{p})) > \mu) \\ &= \mathbb{P}\left(e^{-\|\mathbf{n}\|^2 / 2\sigma^2} < 1 - \frac{\mu}{2}\right) \\ &= \mathbb{P}\left(\sum_{k=1}^K n_k^2 > 2\sigma^2 \log\left(\frac{1}{1 - \frac{\mu}{2}}\right)\right) \end{aligned}$$

where $\mathbf{n} \in \mathbb{R}_+^K$ is a random noise vector with independent exponential random variables $n_k \sim \text{Exp}(\frac{1}{\sigma_n^2})$ (see Sec. II-E).

We would like this probability to be relatively small so that not too many superfluous dictionary items are created as this increases computational complexity.

Exact computation of p_{new} is intractable, but we may upper bound it as:

$$\begin{aligned} p_{\text{new}} &\leq \mathbb{P}\left(K \max_k \{n_k^2\} > 2\sigma^2 \log\left(\frac{1}{1 - \frac{\mu}{2}}\right)\right) \\ &= \mathbb{P}\left(\max_k n_k > \sqrt{\frac{2\sigma^2}{K} \log\left(\frac{1}{1 - \frac{\mu}{2}}\right)}\right) \\ &= 1 - \left(1 - e^{-\frac{1}{\sigma_n^2} \sqrt{\frac{2\sigma^2}{K} \log\left(\frac{1}{1 - \frac{\mu}{2}}\right)}}\right)^K \end{aligned}$$

In order to keep $p_{\text{new}} \leq \delta$ for some small $\delta > 0$ when operating with receiver noise level σ_n^2 , we can choose σ and μ to satisfy the condition:

$$2\sigma^2 \log\left(\frac{1}{1 - \frac{\mu}{2}}\right) > K \left(\sigma_n^2 \log\left(\frac{1}{1 - (1 - \delta)^{1/K}}\right)\right)^2 \quad (6)$$

Equation (6) along with (5) provides an acceptable range of values for the function $\theta = 2\sigma^2 \log\left(\frac{1}{1 - \frac{\mu}{2}}\right)$, and therefore can be used to help choose the parameters σ and μ for a given scenario.

B. Efficient Recursive Implementation

The ALD test may be recursively implemented by avoiding a direct inversion of the kernel matrix \mathbf{K}_{t-1} in (4), which takes $O(L_{t-1}^3)$ computational complexity in general.

If $\delta_t > \mu$, then the new state-action pair $x_t = (s_t, a_t)$ is added to the dictionary and the kernel matrix is updated by adding a new row and column:

$$\mathbf{K}_t = \begin{bmatrix} \mathbf{K}_{t-1} & \mathbf{k}_{t-1}(x_t) \\ \mathbf{k}_{t-1}(x_t)^T & k_{tt} \end{bmatrix}$$

The matrix inverse is then recursively updated as:

$$\mathbf{K}_t^{-1} = \frac{1}{\delta_t} \begin{bmatrix} \delta_t \mathbf{K}_{t-1}^{-1} + \mathbf{c}_t \mathbf{c}_t^T & -\mathbf{c}_t \\ -\mathbf{c}_t^T & 1 \end{bmatrix}$$

with initial value $\mathbf{K}_1^{-1} = [\frac{1}{k_{11}}]$. When implemented using the recursive update, computational complexity to perform the ALD test is reduced to $O(L_{t-1}^2)$.

IV. PERFORMANCE ANALYSIS FOR STATIONARY MARKOV ENVIRONMENTS

In this section we derive the optimal channel access policy for maximizing throughput in unknown environments that can be modeled as a stationary Markov chain. We also derive conditions under which the optimal policy coincides with the maximum-likelihood prediction-and-access policy which is suboptimal in general. For concreteness we consider the noiseless case in this section.

The Markov environments under consideration in this section can be fully characterized by two parameters; the transition probability matrix $\mathbf{P} = \{P_{s,j}\} \in [0, 1]^{N \times N}$ and the connectivity matrix that associates idle channels to states,

$\mathbf{A} = \{A_{j,a}\} \in \{0, 1\}^{N \times K}$. To aide in our exposition define \mathcal{T}_j for $j \in \{1, \dots, N\}$ as sets of indices corresponding to channels that are idle when the system is in state j . Thus, $A_{j,a} = I_{\{a \in \mathcal{T}_j\}}$ where $I_{\{\cdot\}}$ is the indicator function. This is graphically illustrated in Figure 2.

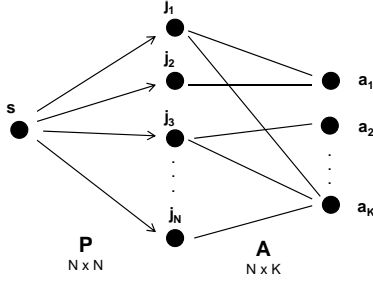


Fig. 2: Graphical model for state transition $s \rightarrow j$ determined by transition matrix \mathbf{P} and connectivity matrix \mathbf{A} associating idle channels (corresp. actions) to states.

The following theorem derives the structure of the optimal policy for average throughput maximization.

Theorem 1. Assume the underlying Markov chain has a finite state space and is irreducible. Let the expected reward after accessing an idle channel a be given by C_a . Consider a randomized policy $\pi^q(s)$ given by:

$$\mathbb{P}(\pi^q(s) = a) = q_a(s)$$

Consider the deterministic policy $\pi^*(s) = \max_a \{C_a \langle P_{s,\cdot}, A_{\cdot,a} \rangle\}$. Then, the policy π^* is optimal and achieves the limiting throughput:

$$\begin{aligned} Thr(\pi^q) &= \lim_{T \rightarrow \infty} \mathbb{E}^{\pi^q} \left[\frac{1}{T} \sum_{t=1}^T r_t \right] \\ &= \sum_{s \in \mathcal{S}} \pi_s \sum_a q_a(s) C_a \langle P_{s,\cdot}, A_{\cdot,a} \rangle \\ &\leq \sum_{s \in \mathcal{S}} \pi_s \max_a \{C_a \langle P_{s,\cdot}, A_{\cdot,a} \rangle\} = Thr(\pi^*) \end{aligned} \quad (7)$$

where π is the stationary distribution of the Markov chain, i.e., $\pi = \pi \mathbf{P}$.

Proof: See Appendix A

We note that Theorem 1 can be generalized to arbitrary action spaces (see Sec.II.B). Theorem 1 provides an upper bound on the average throughput for stationary ergodic Markov environments and characterizes the average throughput optimal policy in terms of an inner product between the rows of \mathbf{P} and the columns of \mathbf{A} .

Another method for choosing an idle channel is the two-stage maximum likelihood (ML) prediction-and-access approach:

- 1) Choose most likely channel to transition to, i.e., $m_s = \arg \max_j P_{s,j}$
- 2) Choose an idle channel a associated with state m_s , i.e., $a \in \mathcal{T}_{m_s}$

According to Theorem 1, this ML policy achieves a sub-optimal throughput. Theorem 2 shows that under some stochastic dominance assumptions, the ML policy coincides with the decisions made by the optimal policy $\pi^*(s) = \max_a \{C_a \langle P_{s,\cdot}, A_{\cdot,a} \rangle\}$.

Theorem 2. Assume all channels have the same capacity, i.e., $C_a = C$. The optimal decision rule makes the same channel access decisions as the ML prediction-and-access algorithm, and thus achieves the same limiting throughput iff:

$$\max_{a \in \mathcal{T}_{m_s}} \left\{ P_{s,m_s} + \sum_{j \neq m_s} P_{s,j} A_{j,a} \right\} > \max_{a \notin \mathcal{T}_{m_s}} \left\{ \sum_{j \neq m_s} P_{s,j} A_{j,a} \right\}, \quad \forall s \in \mathcal{S} \quad (8)$$

where $\mathcal{T}_{m_s} \stackrel{\text{def}}{=} \{a : A_{m_s,a} = 1\}$ and $m_s \stackrel{\text{def}}{=} \arg \max_{j \in \mathcal{S}} P_{s,j}$.

Proof: See Appendix B

Next, we derive expressions for the limiting throughput for the ML prediction-and-access algorithm.

Theorem 3. Assume the underlying Markov chain has a finite state space and is irreducible. Consider the ML prediction-and-access algorithm which chooses a channel $a \in \mathcal{T}_{m_s}$ with probability $q_{m_s}(a)$ when the system is in state s . Let the expected reward after accessing an idle channel a be given by C_a . The limiting throughput is:

$$\begin{aligned} Thr &= \lim_{T \rightarrow \infty} \frac{1}{T} \sum_{t=1}^T r_t \\ &\stackrel{a.s.}{=} \sum_{s \in \mathcal{S}} \pi_s \left(P_{s,m_s} \sum_{a \in \mathcal{T}_{m_s}} q_{m_s}(a) C_a \right. \\ &\quad \left. + \sum_{j \neq m_s} P_{s,j} \sum_{a \in \mathcal{T}_j \cap \mathcal{T}_{m_s}} q_{m_s}(a) C_a \right) \end{aligned} \quad (9)$$

where π is the stationary distribution of the Markov chain, i.e., $\pi = \pi \mathbf{P}$.

The proof of Theorem 3 is similar to the proof of Theorem 1.

The following corollary shows special cases of the ML prediction-and-access decision rule in terms of the state-transition matrix \mathbf{P} and the state-connectivity matrix \mathbf{A} . This result will be used in Section VI to match the empirical results to the theoretical prediction of the throughput.

Corollary 1. The following special cases hold for the ML prediction-and-access decision rule:

- For the case $q_s(a) = I_{\{a=a^*(s)\}}$, where $a^*(s) \stackrel{\text{def}}{=} \arg \max_{a \in \mathcal{T}_{m_s}} C_a$, the expression (9) simplifies to:

$$Thr = \sum_{s \in \mathcal{S}} \pi_s \max_{a \in \mathcal{T}_{m_s}} \{C_a\} \cdot \left(P_{s,m_s} + \sum_{j \neq m_s} P_{s,j} \underbrace{I_{\{a^*(s) \in \mathcal{T}_j\}}}_{=A_{j,a^*(s)}} \right)$$

- For the case when all rewards are equal, i.e., $C_a = C$, and $q_s(a) = \frac{1}{|\mathcal{T}_{m_s}|} I_{\{a \in \mathcal{T}_{m_s}\}}$, the expression (9) becomes:

$$\begin{aligned} Thr &= C \sum_{s \in \mathcal{S}} \pi_s \left(P_{s, m_s} + \sum_{j \neq m_s} P_{s, j} \frac{|\mathcal{T}_j \cap \mathcal{T}_{m_s}|}{|\mathcal{T}_{m_s}|} \right) \\ &= C \sum_{s \in \mathcal{S}} \sum_{j \in \mathcal{S}} \pi_s P_{s, j} \cdot \frac{\sum_{a=1}^K A_{j, a} A_{m_s, a}}{\sum_{a=1}^K A_{m_s, a}} \end{aligned}$$

V. ALGORITHMS

A. Count-based Learning Algorithm

Motivated by the inner-product based optimal decision rule derived in Theorem 1, we propose a recursive count-based learning (CBL) algorithm. CBL attempts to construct the optimal state-action value function (1) using the form given in (2). We show in Theorem 4 that the algorithm asymptotically achieves the optimal throughput given in Theorem 1. The performance of CBL is illustrated using simulation in Section VI-A.

During an initial training period the dictionary of state-action pairs is built using ALD analysis. The α_l corresponding to each state-action pair in the dictionary can be computed as:

$$\begin{aligned} \alpha_l &\stackrel{\text{def}}{=} \alpha_{(s, a)} \\ &= C_a \sum_{j: a \in \mathcal{T}_j} P_{s, j} \end{aligned} \quad (10)$$

where $\mathcal{T}_j = \{a : A_{j, a} = 1\}$ is the set of channels that are idle when the system is in state j , and $P_{s, j}$ is the probability corresponding to the state transition $s \rightarrow j$. Because the radio doesn't have access to the transition statistics of the Markov Chain, $P_{s, j}$ in (10) is replaced by its maximum likelihood estimate:

$$\begin{aligned} \alpha_{(s, a)} &= C_a \sum_{j: a \in \mathcal{T}_j} \frac{N_{s, j}}{N_s} \\ &= C_a \frac{\sum_{j: a \in \mathcal{T}_j} N_{s, j}}{N_s} \end{aligned} \quad (11)$$

where $N_{s, j}$ is the number of observed transitions $s \rightarrow j$, and N_s is the number of observed occurrences of state s . Neglecting the ALD test, a straightforward implementation of this algorithm has per-step computational complexity $O(L)$ and storage complexity $O(N^2)$ where N is the number of unique states in the dictionary, $L \leq |\mathcal{A}|N$ is the total number of entries in the dictionary and $|\mathcal{A}|$ is the cardinality of the action space. Overall computational and storage complexity are dominated by the ALD test described in Section III-B, pushing both to $O(L^2)$.

Because we are interested only in choosing actions and not directly learning \mathbf{P} , we recursively compute (11) and avoid the intermediate step of estimating and storing the transition matrix as follows. Assume the states $(s_{t-1}, s_t) = (i, j)$ are observed. Updating the α_l 's at time t requires updating N_j , $N_{i, j}$ and their dependent α_l 's. Assuming a 1-step latency is acceptable, these updates can be efficiently implemented using the following pair of recursive equations:

$$N_i(t) = N_i(t-1) + 1 \quad (12)$$

$$\begin{aligned} \alpha_{(i, a)}(t) &= \frac{\alpha_{(i, a)}(t-1)N_i(t-1) + r_t I_{\{a \in \mathcal{T}_j\}}}{N_i(t)}, a \in \mathcal{A} \\ &= \frac{r_t}{N_i(t)} I_{\{a \in \mathcal{T}_j\}} + \left(1 - \frac{1}{N_i(t)}\right) \alpha_{(i, a)}(t-1) \end{aligned} \quad (13)$$

where $I_{\{a \in \mathcal{T}_j\}}$ can be computed by observing state $s_t = j$, and r_t is the reward obtained as a result of taking action a_{t-1} in state s_{t-1} . The storage complexity of this update is $O(L)$ and the computational complexity is $O(|\mathcal{A}|)$, which means that the overall complexity of the algorithm is still dominated by the ALD test.

The recursion (13) can alternatively be written in terms of a stochastic approximation update:

$$\alpha_{t+1} = \alpha_t + \text{diag}(N_t)^{-1} \left(r_t - \alpha_t^T \mathbf{k}_t((s_t, a_t)) \right) \mathbf{k}_t((s_t, a_t)) \quad (14)$$

When there is noise present in the channel, a small step size $\eta > 0$ may be used:

$$\alpha_{t+1} = \alpha_t + \eta \left(r_t - \alpha_t^T \mathbf{k}_t((s_t, a_t)) \right) \mathbf{k}_t((s_t, a_t)) \quad (15)$$

The following theorem shows that the CBL decision rule asymptotically achieves the optimal throughput.

Theorem 4. *Let the minimum distance between states in the dictionary be given as $d_{\min}(\mathcal{S}) = \min_{s' \neq s} \|s - s'\|$. Fix $\delta > 0$ to be arbitrarily small, and assume:*

$$\sigma^2 \leq \frac{d_{\min}(\mathcal{S})^2}{2 \ln \left(\frac{N-1}{\delta} \right)} \quad (16)$$

The count-based learning decision rule chooses channel access actions based on the following rule asymptotically:

$$\pi(s) = \arg \max_{a \in \mathcal{A}} \{ \langle P_{s, \cdot}, A_{\cdot, a} \rangle + \epsilon_a \} \quad (17)$$

where $\epsilon_a \in [0, \delta]$. Here, $P_{s, \cdot}$ is the s -th row of the transition probability matrix \mathbf{P} and $A_{\cdot, a}$ is the a -th column of the state-action connectivity matrix \mathbf{A} .

Proof: See Appendix C

We note that while not pursued in this paper, Theorem 4 can be generalized to arbitrary action spaces.

B. Kernel Q-Learning

The Q-learning algorithm [22] seeks to find the policy $\pi(\cdot)$ that maximizes the discounted cumulative reward:

$$\mathbb{E}^\pi \left[\sum_{t=0}^{\infty} \gamma^t r_t \right]$$

where $\gamma \in [0, 1)$ is the discount parameter. This criterion models rewards received sooner as being more important than rewards received later. The Q-learning algorithm estimates the optimal state-action value function Q^* using the stochastic approximation:

$$Q_{t+1}(s_t, a) = Q_t(s_t, a) + \eta \left(r_t + \gamma \max_{a'} Q_t(s_{t+1}, a') - Q_t(s_t, a) \right)$$

Algorithm 1 Kernel R-Learning Algorithm (KRL)

Input: step sizes η, β

Initialize $\rho_0 = 0$

for $t = 1, \dots, T$: **do**

(a) Choose action a_t based on ϵ -greedy policy, i.e.,

$$a_t = \begin{cases} \arg \max_{a \in \mathcal{A}} \alpha_t^T \mathbf{k}_t((s_t, a)), & \text{w.p. } 1 - \epsilon \\ \sim \text{unif}(\mathcal{A}), & \text{w.p. } \epsilon \end{cases}$$

(b) Take action a_t , observe reward r_t and next state s_{t+1}

(c) Update policy

$$\alpha_{t+1} = \alpha_{t-1} + \eta \left(r_t - \rho_t + \max_{a'} \{ \alpha_t^T \mathbf{k}_t((s_{t+1}, a')) \} - \alpha_t^T \mathbf{k}_t((s_t, a_t)) \right) \mathbf{k}_t((s_t, a_t))$$

(d) Update average expected reward per time step:

if $\alpha_t^T \mathbf{k}_t((s_t, a_t)) = \max_a \alpha_t^T \mathbf{k}_t((s_t, a))$ **then**

$$\rho_{t+1} = \rho_t + \beta \left(r_t - \rho_t + \max_{a'} \alpha_t^T \mathbf{k}_t((s_{t+1}, a')) - \max_a \alpha_t^T \mathbf{k}_t((s_t, a)) \right)$$

else

$$\rho_{t+1} = \rho_t$$

end if

end for

In the kernel setting, the Q-learning iteration becomes:

$$\alpha_{t+1} = \alpha_t + \eta \left(r_t + \gamma \max_{a'} \{ \alpha_t^T \mathbf{k}_t((s_{t+1}, a')) \} - \alpha_t^T \mathbf{k}_t((s_t, a_t)) \right) \mathbf{k}_t((s_t, a_t))$$

C. Kernel R-Learning

To maximize throughput, we want to maximize the following undiscounted average reward:

$$\rho^\pi = \lim_{n \rightarrow \infty} \frac{1}{n} \sum_{t=1}^n \mathbb{E}^\pi [r_t]$$

instead of the discounted cumulative reward. For γ approaching 1, this maximization approaches the average cost criterion. The R-learning algorithm of Schwartz [25] maximizes the average adjusted sum of rewards:

$$Q^\pi(s, a) = \sum_{k=1}^{\infty} \mathbb{E}^\pi [r_{t+k} - \rho^\pi | s_t = s, a_t = a]$$

It is based on iteratively solving for a fixed point of the Bellman equation [26]

$$Q^*(s, a) + \rho^* = r(s, a) + \sum_{s'} P_{s, s'}(a) \max_{a'} Q^*(s', a')$$

where ρ^* is the average reward for the optimal policy. The stochastic approximation algorithm is shown in Alg. 1 for the kernel setting. A numerical study comparing Q-learning with R-learning was conducted in [27] and it is shown that R-learning can outperform Q-learning.

D. Generalized Kernel R-Learning

The CBL method computes a set of coefficients α_t using (15) to maximize the single-stage expected reward. To speed up learning, we may choose actions by maximizing the difference between the R-learning and CBL value functions. Of course, in order for the modified algorithm to approach the solution obtained with R-learning, the effect of the CBL single-stage value function in the decision making is damped down by the number of times that action has been chosen when the system is in that state, $N_t(s_t, a)$. This idea of guided action selection to maximize the future reward when in the transient regime has the potential of speeding up convergence.

In our proposed Generalized Kernel-based R-Learning (GKRL) approach actions are chosen as:

$$a_t = \begin{cases} \arg \max_a \left\{ \alpha_t^T \mathbf{k}_t((s_t, a)) - \frac{\tilde{\alpha}_t^T \mathbf{k}_t((s_t, a))}{N_t(s_t, a)^{1+\zeta}} I_t^+ \right\}, & \text{w.p. } 1 - \epsilon \\ \sim \text{unif}(\mathcal{A}), & \text{w.p. } \epsilon \end{cases}$$

where $\zeta \geq 0$,

$$I_t^+ \stackrel{\text{def}}{=} \begin{cases} 1, & \max_a \{ \alpha_t^T \mathbf{k}_t((s_t, a)) - \tilde{\alpha}_t^T \mathbf{k}_t((s_t, a)) \} \geq 0 \\ 0, & \text{else} \end{cases},$$

$$N_t(s_t, a) \stackrel{\text{def}}{=} \sum_{(s', a') \in \mathcal{D}_t: \|s' - s_t\| < \delta, a' = a} \text{cnts}_t(s', a')$$

and $\tilde{\alpha}_t$ is the vector of coefficients computed using (14). Here, $\text{cnts}_t(s_t, a)$ estimates the number of times action a has been chosen when the system is in state s_t and is computed as:

$$\text{cnts}_t(s, a) = \sum_{i=1}^t k((s_i, a_i), (s, a))$$

for all (s, a) pairs in the dictionary. The threshold δ is based on the noise variance and attempts to cluster similar states.

We remark that in the large sample regime, we expect $N_t(s_t, a) \rightarrow \infty$ and the GKRL method behaves identically as KRL. However, in the transient regime where most learning occurs on startup, the algorithm seeks to choose actions that maximize the gap between the expected long-term average reward and the expected myopic reward.

VI. NUMERICAL EXPERIMENTS

A. Simulated Data

1) *Setup:* To compare the performance of the proposed algorithms we simulate a scenario in which a pair of full-duplex blue cognitive network radios attempt to operate in the presence of K green network radio links. We assume that the green network is non-cooperative with the blue network. Each of the K green links consists of a pair of transceivers communicating over a channel with line-of-sight (LOS) propagation loss. The K channels are assumed to be non-overlapping in frequency and each has of bandwidth of W Hz. We make the simplifying assumption that the channels can be decomposed into time slots of duration T_{slot} . Each of the blue network radios is constrained to access the one of the same K W Hz channels being used by the green network and must attempt to minimize collisions. Blue and green network

Parameter	Value (units)	Description
K	5 (links or channels)	number of available channels
W	1.2 (MHz)	bandwidth of each channel
R	600 (kbits/sec)	maximum data rate of each link
T_{slot}	1.5 (ms)	channel access duration
P_{gtx}	20 (dBm)	green network transmit power

TABLE I: Parameters used in numerical experiments

radios are assumed to operate at a rate of R bits/sec² when no collisions occur. The values of each of the parameters chosen for our numerical experiments are summarized in Table (I). Throughout our experiments the radio links are configured in a particular randomly generated physical layout as shown in Figure (3).

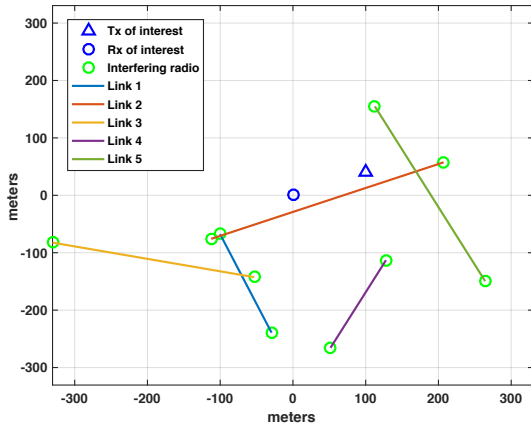


Fig. 3: Physical layout of the blue and green networks. Each link is denoted by a line connecting a transceiver pair. The states are generated assuming line-of-sight pathloss between each of the green network radios and the blue network receiver of interest.

For our simulations the composite channel evolves in time according to a ergodic first-order Markov Chain over 10 randomly generated states. The state space is shown in Figure (4).

Prior to being processed by any of the learning algorithms, the observed power measurements are normalized by mapping them to the unit interval. This helps with numerical stability.

We characterize performance of each algorithm in both stationary and reactive settings. In the stationary case, the green network is not affected by the actions being taken by the blue network, while for the reactive case, the green network adapts to the blue network's actions. We compare our algorithms with collision avoidance (CA) which consists of sensing, finding an idle channel and accessing it in the next time slot.

2) *Performance*: The metric we use is the average throughput as a function of training time, which characterizes the learning performance of each algorithm. In our simulation, each sample corresponds to 1.5ms. Monte Carlo simulations are performed where the training set was generated randomly over many trials, and for each trial the optimal policy was learned using the nonparametric learning techniques developed

²Specifically, each radio operates at the Nyquist rate of its respective channel using a 1/2 rate code and antipodal signaling.

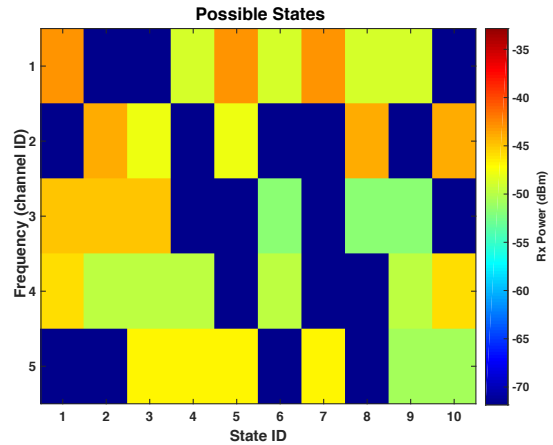


Fig. 4: The channel is modeled as a 1st-order Markov Chain with 10 possible channel states. The columns of the above image illustrate each of these states as observed at the blue network receiver.

and performance was averaged over many trials on heldout sets to obtain the average throughput.

a) *Stationary Case*: We compare the CBL method with maximum-likelihood (ML) prediction and access. We consider the transition probability matrix \mathbf{P} shown in Fig. 5. Each row of this matrix consists of a single dominant probability of jumping to some randomly chosen next state while the remaining probabilities are uniformly chosen to sum to unity. Fig. 6 shows the achievable throughput as a function of training time for both noiseless and noisy channels. Both CBL and ML methods outperform CA and CBL achieves the optimal throughput 366Kbps as expected from Theorem 1, while ML achieves a suboptimal throughput of 347Kbps. Fig.

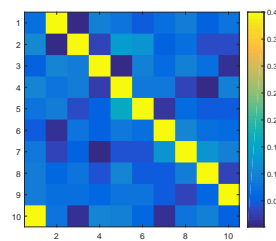


Fig. 5: Probability transition matrix used for stationary example.

7 shows the histogram of the normalized powers over a block of noisy data. We note the noise is exponentially distributed as discussed in Section II-E.

b) *Reactive Case*: We compare the modified CBL algorithm, Kernel Q-learning (KQL), Kernel R-learning (KRL) and Generalized Kernel R-learning (GKRL) for the probability matrices $\mathbf{P}(a)$ shown in Fig. 8. These matrices were designed so that the optimal single-stage reward over two stages is suboptimal with respect to the optimal two-stage reward. The optimal policy here is a two-stage policy given by $\pi^*(s) = \sum_{k=1}^{10} a_k I_{\{s=k\}}$, $\mathbf{a} = [3, 3, 4, 5, 5, 3, 3, 4, 5, 5]$ and the suboptimal single-stage policy is $\pi^G(s) = \sum_{k=1}^{10} b_k I_{\{s=k\}}$, $\mathbf{b} = [1, 2, 3, 4, 5, 1, 2, 3, 4, 5]$. Actions that lead to channel 5 or 10 being chosen are desirable since these two channels have triple

the bandwidth of the rest of the channels and thus yield a higher reward when accessed in an idle state.

Online performance refers to the throughput obtained while learning which involves taking random actions to explore with probability ϵ , while offline performance refers to the throughput obtained when actions are chosen based on maximizing the Q function and thus no exploration is performed. Figures 9 and 10 show the mean and standard deviation of the throughput when 100 Monte Carlo trials are performed for the noiseless case. The online performance is lower than the offline performance because a random action is taken for exploration with probability $\epsilon = 0.1$ in the former. We observe that KRL and GKRL both achieve the optimal throughput 1000Kbps, while KQL with $\gamma = 0.99$ and CBL only achieve a throughput of approximately 750Kbps. It is interesting how even with a γ close to unity, KQL does not achieve the optimal throughput. Finally, GKRL approaches maximum performance faster than KRL in both the online and offline settings.

Figures 11 and 12 show the mean and standard deviation of the average throughput for the case with channel noise. In this case the receiver of interest observes the green network

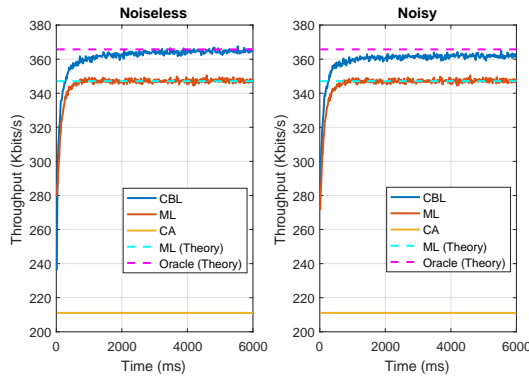


Fig. 6: Stationary case. Throughput as a function of training time for noiseless and noisy cases. CBL achieves the optimal throughput as predicted by theory, and ML achieves a suboptimal throughput. CBL achieves a throughput $\times 1.7$ larger than CA.

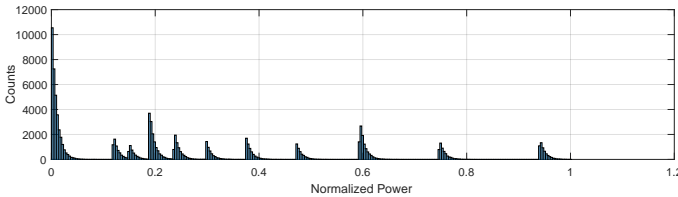


Fig. 7: Histogram of normalized power levels in the presence of noise.

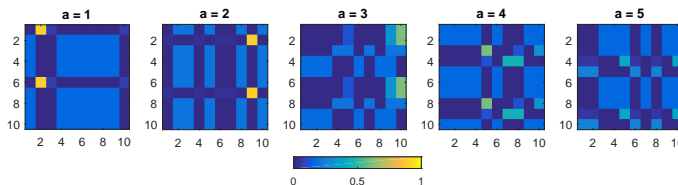


Fig. 8: Probability transition matrices used for the reactive example.

radios at various signal-to-noise ratios ranging from 11 to 20dB depending on relative pathloss. Both GKRL and KRL methods achieve the optimal throughput 1000Kbps, while KQL achieves a throughput of 750Kbps and CBL achieves a throughput of 800Kbps. We note that even when there is noise present, GKRL continues to learn faster than KRL. Furthermore, GKRL has smaller fluctuations around its mean as it has a lower standard deviation.

B. Reactive MAC Layer Results

In this section, a reactive green network competes with the blue cognitive network running a reinforcement learning algorithm and average throughput performance is evaluated. The green network MAC layer is intuitive and is based on reacting to the blue network's actions while at the same time trying to increase its throughput. The goal of the blue cognitive radio network is to create and exploit white space opportunities by learning the behavior of the green network and reacting to it appropriately to increase its throughput.

The green network's behavior is outlined in Fig. 13, which describes the probabilistic evolution of each subchannel. The green network does not attempt to learn the behavior of the

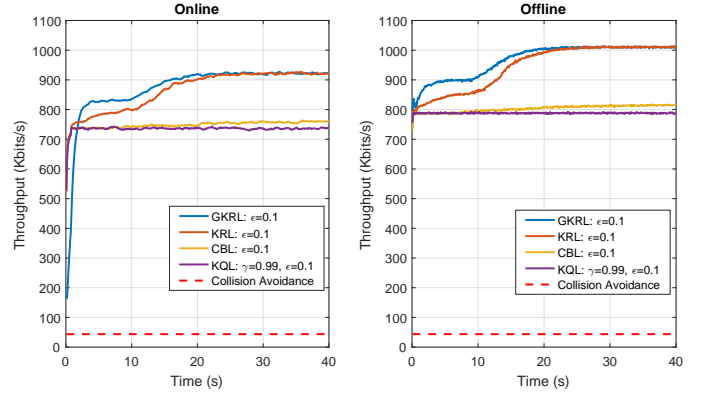


Fig. 9: Reactive noiseless case. Mean throughput averaged over 100 trials as a function of time in online (left panel) and offline (right panel) setting. GKRL outperforms all algorithms in terms of achievable throughput and learning rate.

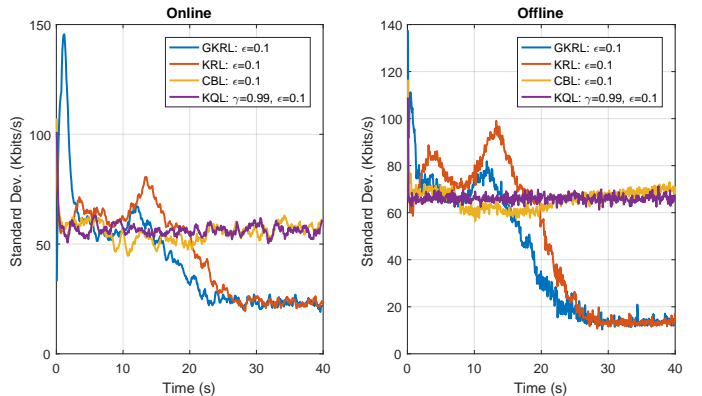


Fig. 10: Reactive noiseless case. Standard deviation of throughput averaged over 100 trials as a function of time. GKRL has the lowest asymptotic variance.

blue network. Instead, the probabilities p and q determine how the network reacts to interference in each subchannel, while the probability z determines the likelihood of the green network beginning to access an idle subchannel when no interference is present. Note that as $(p, q) \rightarrow (1, 0)$ the green network can be characterized as highly competitive, as it attempts to minimize channel access by blue network radios. For $(p, q) \rightarrow (0, 1)$ the network becomes less competitive, as it is less likely to attempt to block access and more likely to yield use of a subchannel to a blue network radio.

We consider the case when the blue cognitive network may access at most two of the $K = 5$ channels at a time, yielding a total number of actions $K + \binom{K}{2} = 15$. This allows for higher throughput and also allows for the possibility of one action to be exploratory in nature while the other action is exploitative. Figure 14 shows the throughput as a function of training time in the presence of noise. In this simulation, we used $p = 0.2, q = 0.9, z = 0.5$ to model the reactive green network. The GKRL method outperforms all in terms of throughput when exploring and when not exploring. The GKRL method asymptotically achieves the highest throughput of 1020Kbps while the KQL method with $\gamma = 0.99$ and

CBL lag significantly behind at 900Kbps. Furthermore, GKRL achieves a throughput at least $\times 2$ larger when compared to collision avoidance. Figure 15 also shows that GKRL and KRL methods achieve the lowest variance asymptotically. It is interesting that GKRL has a lower variance than KRL throughout the learning process.

VII. CONCLUSION

We propose low-complexity nonparametric learning algorithms for reinforcement learning over large and continuous

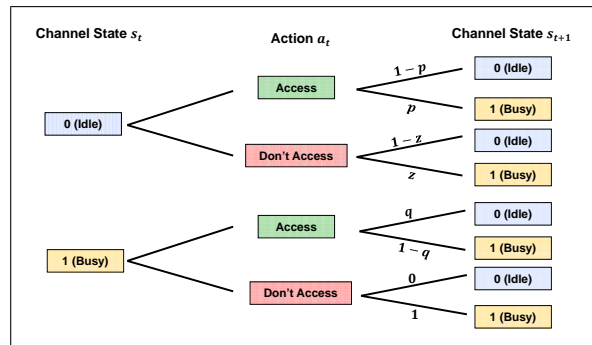


Fig. 13: Probabilistic MAC layer diagram. The next channel state s_{t+1} depends on the previous channel state s_t and the action taken a_t .

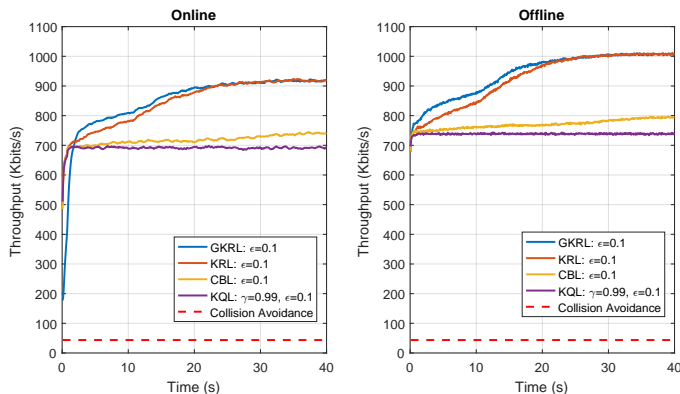


Fig. 11: Reactive noisy case. Mean throughput averaged over 100 trials as a function of time in online (left panel) and offline (right panel) setting. GKRL outperforms all algorithm in terms of achievable throughput and learning rate.

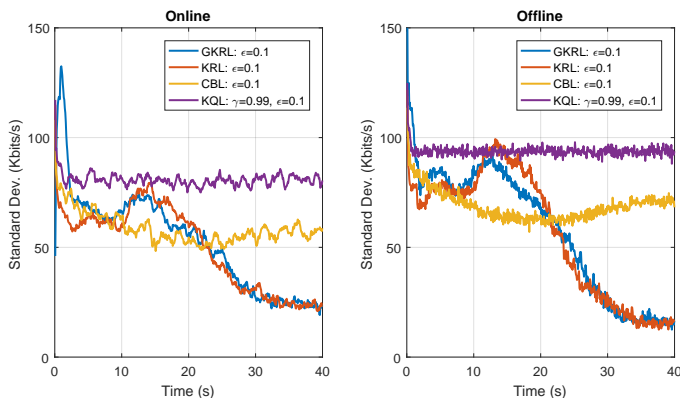


Fig. 12: Reactive noisy case. Standard deviation of throughput averaged over 100 trials as a function of time. GKRL and KRL have the lowest asymptotic variance.

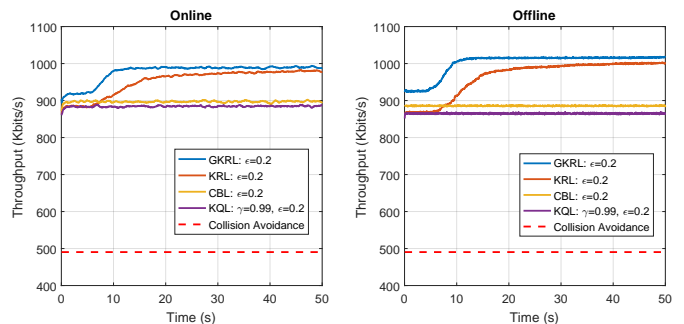


Fig. 14: Mean throughput of blue cognitive network in presence of reactive green network with MAC layer (see Fig. 13) averaged over 100 trials as a function of training time. GKRL outperforms all methods asymptotically.

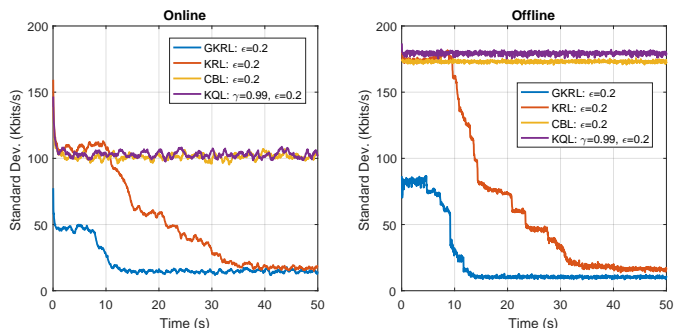


Fig. 15: Standard deviation of throughput of blue cognitive network in presence of reactive green network with MAC layer (see Fig. 13) averaged over 100 trials. GKRL achieves the lowest asymptotic variance.

state spaces. For stationary environments, we also derive bounds on the achievable throughput and derive conditions under which the maximum-likelihood prediction achieves the optimal performance. Kernel variants of Q-learning, R-learning were derived, in addition to a novel accelerated R-learning algorithm for learning optimal channel access policies in reactive environments. Simulation results show the benefits of our approach over Q-learning and collision avoidance schemes.

APPENDIX A PROOF OF THEOREM 1

Proof. Since the Markov chain is irreducible with finite state space, it is also positive recurrent and a stationary distribution π exists and is the unique solution to $\pi = \pi \mathbf{P}$. The average reward under policy π^q after T steps is given by:

$$\begin{aligned} \mathbb{E}^{\pi^q} \left[\frac{1}{T} \sum_{t=1}^T r_t \right] &= \frac{1}{T} \sum_{t=1}^T \sum_{s \in \mathcal{S}} I_{\{s_t=s\}} \mathbb{E}^{\pi^q} [r_t | s_t = s] \\ &= \frac{1}{T} \sum_{t=1}^T \sum_s I_{\{s_t=s\}} \sum_j P_{s,j} \mathbb{E}[r_t | s_t = s, s_{t+1} = j] \\ &= \frac{1}{T} \sum_{t=1}^T \sum_s I_{\{s_t=s\}} \sum_j P_{s,j} \\ &\quad \times \sum_a q_a(s) \mathbb{E}[r_t | s_t = s, a_t = a, s_{t+1} = j] \\ &= \frac{1}{T} \sum_{t=1}^T \sum_s I_{\{s_t=s\}} \sum_j P_{s,j} \sum_a q_a(s) A_{j,a} C_a \\ &= \sum_s \left(\frac{1}{T} \sum_{t=1}^T I_{\{s_t=s\}} \right) \sum_j P_{s,j} \sum_a q_a(s) A_{j,a} C_a \end{aligned}$$

Using the following asymptotic results for Markov chains:

$$\frac{1}{T} \sum_{t=1}^T I_{\{s_t=s\}} \xrightarrow{a.s.} \pi_s$$

we obtain:

$$\begin{aligned} \text{Thr}(\pi^q) &= \sum_s \pi_s \sum_j P_{s,j} \left(\sum_a q_a(s) A_{j,a} C_a \right) \\ &= \sum_s \pi_s \sum_a q_a(s) \left(\sum_j P_{s,j} A_{j,a} \right) C_a \\ &= \sum_s \pi_s \sum_a q_a(s) \langle P_{s,\cdot}, A_{\cdot,a} \rangle C_a \\ &\leq \sum_s \pi_s \max_a \{ \langle P_{s,\cdot}, A_{\cdot,a} \rangle C_a \} \end{aligned}$$

The policy π^* achieves the upper bound. The proof is complete. \square

APPENDIX B PROOF OF THEOREM 2

Proof. The ML algorithm chooses an action $a \in \mathcal{T}_{m_s}$, where m_s is the most likely state transition starting from state

s . From Theorem 4, the optimal decision rule chooses an action that maximizes the inner product $\langle P_{s,\cdot}, A_{\cdot,a} \rangle$. Notice the following:

$$\begin{aligned} \langle P_{s,\cdot}, A_{\cdot,a} \rangle &= P_{s,m_s} + \sum_{j \neq m_s} P_{s,j} A_{j,a}, \quad \text{for } a \in \mathcal{T}_{m_s} \\ \langle P_{s,\cdot}, A_{\cdot,a} \rangle &= \sum_{j \neq m_s} P_{s,j} A_{j,a}, \quad \text{for } a \notin \mathcal{T}_{m_s} \end{aligned}$$

Under the conditions (8), the maximum inner product decision rule (17) always chooses an action $a \in \mathcal{T}_{m_s}$, which coincides with the ML decision rule.

Next suppose that (8) is violated for a particular state $s \in \mathcal{S}$. Then, $\max_{a \in \mathcal{T}_{m_s}} \{ P_{s,m_s} + \sum_{j \neq m_s} P_{s,j} A_{j,a} \} \leq \max_{a \notin \mathcal{T}_{m_s}} \{ \sum_{j \neq m_s} P_{s,j} A_{j,a} \}$, and the inner product decision rule (17) may yield an $a \notin \mathcal{T}_{m_s}$. Thus, the converse also holds. The proof is complete. \square

APPENDIX C PROOF OF THEOREM 4

Proof. The coefficients converge to:

$$\alpha_{(s,a)} = \sum_{j: A_{j,a} \neq 0} \frac{N_{s,j}}{N_s} \rightarrow \sum_{j: A_{j,a} \neq 0} P_{s,j} = \langle P_{s,\cdot}, A_{\cdot,a} \rangle$$

where the dictionary $\mathcal{D} = \{(s_l, a_l)\}_{l=1}^L$ has size $L = |\mathcal{D}|$. The decision rule asymptotically becomes:

$$\pi(s) = \arg \max_{a \in \mathcal{A}} \left\{ Q(s, a) = \sum_{l=1}^L \alpha_{(s_l, a_l)} k((s, a), (s_l, a_l)) \right\} \quad (18)$$

Consider a particular state s that exists in the dictionary \mathcal{D} . Then, the Q-function may be decomposed as:

$$\begin{aligned} Q(s, a) &= \sum_{s_l=s} \alpha_{(s_l, a_l)} e^{-\frac{(a-a_l)^2}{2\sigma^2}} + \sum_{s_l \neq s} \alpha_{(s_l, a_l)} e^{-\frac{\|s-s_l\|^2}{2\sigma^2}} e^{-\frac{(a-a_l)^2}{2\sigma^2}} \\ &= \sum_{s_l=s} \langle P_{s,\cdot}, A_{\cdot, a_l} \rangle e^{-\frac{(a-a_l)^2}{2\sigma^2}} \\ &\quad + \sum_{s_l \neq s} \langle P_{s_l, \cdot}, A_{\cdot, a_l} \rangle e^{-\frac{\|s-s_l\|^2}{2\sigma^2}} e^{-\frac{(a-a_l)^2}{2\sigma^2}} \\ &= \sum_{k=1}^K c(s, k) e^{-\frac{(a-k)^2}{2\sigma^2}} \end{aligned}$$

where the coefficients are

$$c(s, k) = \langle P_{s,\cdot}, A_{\cdot, k} \rangle + \sum_{s_l \neq s} \langle P_{s_l, \cdot}, A_{\cdot, k} \rangle e^{-\frac{\|s-s_l\|^2}{2\sigma^2}}$$

The inequality (16) guarantees that:

$$\langle P_{s,\cdot}, A_{\cdot, k} \rangle \leq c(s, k) \leq \langle P_{s,\cdot}, A_{\cdot, k} \rangle + \delta$$

since

$$\begin{aligned} \sum_{s_l \neq s} \langle P_{s_l, \cdot}, A_{\cdot, k} \rangle e^{-\frac{\|s-s_l\|^2}{2\sigma^2}} &\leq \sum_{s_l \neq s} \|P_{s_l, \cdot}\|_1 \|A_{\cdot, k}\|_\infty e^{-\frac{\|s-s_l\|^2}{2\sigma^2}} \\ &= \sum_{s_l \neq s} e^{-\frac{\|s-s_l\|^2}{2\sigma^2}} \leq (N-1) \max_{s' \neq s} e^{-\frac{\|s-s'\|^2}{2\sigma^2}} \\ &= (N-1) e^{-\frac{d_{\min}(s)}{2\sigma^2}} \leq \delta \end{aligned}$$

For small enough δ , $c(s, k) \approx \langle P_{s,\cdot}, A_{\cdot,k} \rangle$, and the decision rule (18) coincides with (17). \square

REFERENCES

- [1] FCC Spectrum Policy Task Force, "Report of the spectrum efficiency working group," November 2002.
- [2] Q. Zhao and B. M. Sadler, "A survey of dynamic spectrum access: processing, networking, and regulatory policy," *IEEE Signal Processing Magazine*, vol. 24, no. 3, pp. 79–89, May 2007.
- [3] P. D. Sutton, J. Lotze, H. Lahlou, B. Ozgul, S. A. Fahmy, K. E. Nolan, J. Noguera, and L. E. Doyle, "Multi-platform demonstrations using the Iris architecture for cognitive radio network testbeds," in *International Conf. Cognitive Radio Oriented Wireless Networks and Commun.*, 2010.
- [4] D. Xu, Q. Zhang, Y. Liu, Y. Xu, and P. Zhang, "An Architecture for Cognitive Radio Networks with Cognition, Self-Organization and Reconfiguration Capabilities," in *IEEE Vehicular Technology Conference (VTC)*, 2012.
- [5] S. Soltani, Y. Sagduyu, Y. Shi, J. Li, J. Feldman, and J. Matyjas, "Distributed Cognitive Radio Network Architecture, SDR implementation and Emulation Testbed," in *IEEE Military Communications Conference (MILCOM)*, 2015.
- [6] H. Wang, H. Zhao, J. Li, S. Wang, and J. Wei, "Network architecture self-adaptation technology in cognitive radio networks," in *IEEE International Symp. Personal, Indoor, and Mobile Radio Commun. (PIMRC)*, 2016.
- [7] D. B. Rawat, "Roar: An architecture for real-time opportunistic spectrum access in cloud-assisted cognitive radio networks," in *IEEE Consumer Commun. & Networking Conf. (CCNC)*, 2016.
- [8] Q. Zhao, L. Tong, A. Swami, and Y. Chen, "Decentralized cognitive MAC for opportunistic spectrum access in ad hoc networks: a POMDP framework," *IEEE J. Sel. Areas Commun.*, vol. 17, no. 4, pp. 589–600, April 2007.
- [9] Y. Chen, Q. Zhao, and A. Swami, "Joint design and separation principle for opportunistic spectrum access in the presence of sensing errors," *IEEE Trans. Inf. Theory*, vol. 54, no. 5, pp. 2053–2071, May 2008.
- [10] Q. Zhao, B. Krishnamachari, and Y. Chen, "On myopic sensing for multichannel opportunistic access: structure, optimality, and performance," *IEEE Trans. Wireless Commun.*, vol. 7, no. 12, pp. 5431–5440, December 2008.
- [11] Q. Zhao, S. G. adn L. Tong, and B. M. Sadler, "Opportunistic spectrum access via periodic channel sensing," *IEEE Trans. Signal Processing*, vol. 56, no. 2, pp. 785–796, February 2008.
- [12] M. Derakhshani and T. Le-Ngoc, "Learning-based opportunistic spectrum access with adaptive hopping transmission strategy," *IEEE Trans. Wireless Commun.*, vol. 11, no. 11, pp. 3957–3967, Nov. 2012.
- [13] S. K. Jayaweera, *Signal Processing for Cognitive Radios*. John Wiley & Sons, Inc., 2015.
- [14] D. W. Browne, "Predicting communications activity in the radio spectrum," in *Asilomar Conf. Signals, Systems and Computers*, 2012.
- [15] V. Tumuluru, P. Wang, and D. Niyato, "Channel status prediction for cognitive radio networks," *Wireless Communications and Mobile Computing*, vol. 12, pp. 862–874, 2012.
- [16] A. Nguyen, J. Yosinski, and J. Clune, "Deep Neural Networks are Easily Fooled: High Confidence Predictions for Unrecognizable Images," in *IEEE Conf. Computer Vision and Pattern Recognition (CVPR)*, 2015, pp. 427–436.
- [17] N. Papernot, P. McDaniel, S. Jha, M. Fredrikson, Z. B. Celik, and A. Swami, "The Limitations of Deep Learning in Adversarial Settings," in *IEEE European Symposium on Security and Privacy*, 2016, pp. 372–387.
- [18] B. F. Lo and I. F. Akyildiz, "Reinforcement learning for cooperative sensing gain in cognitive radio ad hoc networks," *Wireless Networks*, vol. 19, pp. 1237–1250, 2013.
- [19] A. Galindo-Serrano and L. Giupponi, "Distributed Q-Learning for aggregated interference control in cognitive radio networks," *IEEE Transactions on Vehicular Technology*, vol. 59, no. 4, pp. 1823–1834, May 2010.
- [20] L. Wang and V. Fodor, "Dynamic Cooperative Secondary Access in Hierarchical Spectrum Sharing Networks," *IEEE Transactions on Wireless Communications*, vol. 13, no. 114, pp. 6068–6080, November 2014.
- [21] N. Morozs, T. Clarke, and D. Grace, "Distributed Heuristically Accelerated Q-Learning for robust cognitive spectrum management in LTE cellular systems," *IEEE Transactions on Mobile Computing*, vol. 15, no. 4, pp. 817–825, April 2016.
- [22] R. S. Sutton and A. G. Barto, *Reinforcement Learning : An Introduction*. MIT Press, 1998.
- [23] X. Xu, D. Hu, and X. Lu, "Kernel-Based Least Squares Policy Iteration for Reinforcement Learning," *IEEE Transactions on Neural Networks*, vol. 18, no. 4, pp. 973–992, July 2007.
- [24] Y. Engel, S. Mannor, and R. Meir, "The Kernel Recursive Least-Squares Algorithm," *IEEE Transactions on Signal Processing*, vol. 52, no. 8, pp. 2275–2285, August 2004.
- [25] A. Schwartz, "A Reinforcement Learning method for maximizing undiscounted rewards," in *International Conference on Machine Learning*, 1993.
- [26] S. P. Singh, "Reinforcement Learning Algorithms for Average-Payoff Markovian Decision Processes," in *AAAI National Conference on Artificial Intelligence*, 1994.
- [27] S. Mahadevan, "Average Reward Reinforcement Learning: Foundations, Algorithms, and Empirical Results," *Machine Learning*, vol. 22, pp. 159–195, 1996.